
Rethinking Irregular Time Series Forecasting: A Simple yet Effective Baseline

Xvyuan Liu*, Xiangfei Qiu*, Xingjian Wu, Zhengyu Li, Chenjuan Guo, Jilin Hu^{1†}, Bin Yang

Abstract

The forecasting of irregular multivariate time series (IMTS) is crucial in key areas such as healthcare, biomechanics, climate science, and astronomy. However, achieving accurate and practical predictions is challenging due to two main factors. First, the inherent irregularity and data missingness in irregular time series make modeling difficult. Second, most existing methods are typically complex and resource-intensive. In this study, we propose a general framework called APN to address these challenges. Specifically, we design a novel Time-Aware Patch Aggregation (TAPA) module that achieves adaptive patching. By learning dynamically adjustable patch boundaries and a time-aware weighted averaging strategy, TAPA transforms the original irregular sequences into high-quality, regularized representations in a channel-independent manner. Additionally, we use a simple query module to effectively integrate historical information while maintaining the model’s efficiency. Finally, predictions are made by a shallow MLP. Experimental results on multiple real-world datasets show that APN outperforms existing state-of-the-art methods in both efficiency and accuracy.

1 Introduction

Irregular Multivariate Time Series (IMTS) data are widely observed in various domains such as healthcare, biomechanics, climate science, and astronomy [Yao et al., 2018, Brouwer et al., 2019, Kidger et al., 2020, Ham et al., 2019, Vio et al., 2013]. Irregular Multivariate Time Series Forecasting (IMTSF) is a crucial research task that provides valuable insights for early warning and proactive decision-making. However, the inherent irregularity of observations and data missingness [Yalavarthi et al., 2024, Zhang et al., 2024] in IMTS pose significant challenges to IMTSF modeling.

To address this challenge, recent IMTSF methods, such as T-PatchGNN [Zhang et al., 2024] and TimeCHEAT [Liu et al., 2025], have adopted the Fixed Patching approach—see Figure 1a. This approach divides the time series into fixed-length patches with equal intervals among them. However, this approach has notable limitations: 1) *Uneven Information Density Across Patches*: Fixed Patching struggles to adapt to local variations in data density, leading to uneven information density among patches. For example, sparse patches (where the number of observations is limited) may result in insufficient feature extraction, yet dense patches (where the number of observations is abundant) may contain redundant information or noise, thereby impairing the extracted features. 2) *Inappropriate Segmentation of Key Semantic Information*: Fixed Patching risks splitting critical dynamic information, which hampers the model’s ability to capture the complete semantic context. Therefore, **the first challenge is: how to design an adaptive patching approach** that can adapt to the local information density variations of IMTS and capture complete semantic information.

Meanwhile, existing IMTSF models generally suffer from high computational costs and long running times. For example, neural ODEs-based models [Chen et al., 2018, Rubanova et al., 2019, Gravina et al., 2024] require computationally intensive numerical solvers to accurately model continuous-time dynamics [Shukla and Marlin, 2021, Chen et al., 2018]. GNNs-based models [Yalavarthi et al., 2024, Zhang et al., 2024] are hindered by the overhead of complex

graph construction and multi-round node information aggregation [Wu et al., 2021]; Transformer-based models [Chen et al., 2023, Zhang et al., 2023], which utilize multi-layer self-attention mechanisms and feedforward networks, often result in large parameter scales [Kim et al., 2024]. These models typically construct computationally intensive and parameter-heavy complex architectures to effectively handle the intricate dependencies and dynamic changes in IMTS. While this design enhances the model’s performance to some extent, it also incurs high computational costs and long runtimes, limiting its practical application in resource-constrained scenarios. Notably, in regular time series forecasting task, models such as DLinear [Zeng et al., 2023], SparseTSF [Lin et al., 2024a], and CycleNet [Lin et al., 2024b] have significantly reduced computational overhead and achieved competitive prediction accuracy by adopting simple architectures with fewer parameters. Therefore, **the second challenge is: how to design an effective model for IMTSF.**

To address the above challenges, we propose a general framework called APN. Specifically, we design a novel Time-Aware Patch Aggregation (TAPA) module that achieves adaptive patching—see Figure 1b. By learning dynamically adjustable patch boundaries and a time-aware weighted averaging strategy, TAPA transforms the original irregular sequences into high-quality, regularized representations in a channel-independent manner. Based on the representations, we use a simple query module to effectively integrate historical information while maintaining the model’s efficiency. Finally, predictions are made by a shallow MLP. Results on multiple real-world datasets show that APN outperforms existing state-of-the-art methods in both efficiency and accuracy.

The contributions of our paper are summarized as follows:

- To address the IMTSF, we propose a general framework named APN. This framework leverages adaptive patching to generate high-quality and regular initial patch representations. Based on these representations, we employ a simple query module to integrate contextual information, ensuring the effective design of the framework.
- We design a novel TAPA module to achieve adaptive patching. By learning dynamically adjustable patch boundaries and a time-aware weighted averaging strategy, TAPA transforms the original irregular sequence into high-quality, regularized representations in a channel-independent manner, effectively adapting to local variations in information density and capturing complete semantics.
- We conduct extensive experiments on multiple datasets. The results show that APN outperforms existing SOTA baselines in both forecasting accuracy and computational efficiency.

2 Related Work

2.1 Irregular Multivariate Time Series Forecasting

IMTSF is crucial for key domains such as healthcare and climate science. The inherent characteristics of IMTS, such as non-uniform sampling intervals and asynchronous channels, present significant challenges to regular time series forecasting models. To address these characteristics, researchers have proposed various IMTSF models. Some models employ approaches based on continuous-time dynamics [Chen et al., 2018, Rubanova et al., 2019, Schirmer et al., 2022, Brouwer et al., 2019], utilizing ordinary or stochastic differential equations (ODE/SDE) to adapt to irregular sampling points. For instance, Neural Flows [Bilos et al., 2021] proposes directly modeling the solution curves of ODEs, thereby avoiding the costly numerical integration steps in traditional ODE solvers. GRU-ODE-Bayes [Brouwer et al., 2019] innovatively combines the idea of Gated Recurrent Units (GRU) with ODEs and effectively handles sparse observational data through a Bayesian update mechanism. Other models leverage graph neural networks and attention mechanisms [Yalavarthi et al., 2024, Zhang et al., 2024, Liu et al., 2025] to capture complex dependencies in IMTS. For example, GraFITi [Yalavarthi et al., 2024] transforms IMTS into sparse bipartite graphs and predicts edge weights through GNNs.

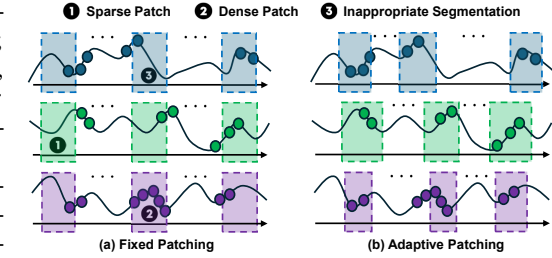


Figure 1: Fixed Patching vs. Adaptive Patching.

T-PatchGNN [Zhang et al., 2024] innovatively segments irregular sequences into time-aligned patches and combines Transformer and adaptive GNNs to handle intra-patch and inter-patch dependencies, respectively.

2.2 Progress in Patch-based Irregular Multivariate Time Series Forecasting

Segmenting time series into “patches” to capture local patterns has demonstrated remarkable success in regular time series forecasting tasks, as evidenced by models like PatchTST [Nie et al., 2023] and Crossformer [Wang et al., 2022]. Inspired by this, the patch-based approach has also been applied to IMTSF. T-PatchGNN [Zhang et al., 2024] employs its “Transformable Patch” mechanism to convert irregular sequences into patches with uniform temporal resolution but variable lengths, thereby maintaining temporal alignment while adapting to the sparsity and density variations of observation points. Meanwhile, TimeCHEAT [Liu et al., 2025] divides IMTS into fixed-length patches and utilizes graph learning within each patch for fine-grained temporal embedding. Both methods ingeniously leverage the patch strategy to transform raw IMTS data into structured representations that are more amenable to model processing, laying the groundwork for subsequent sequence modeling.

Unlike the fixed patching methods mentioned above, this study introduces adaptive patching. By learning dynamically adjustable patch boundaries and employing a time-aware weighted averaging strategy, our method transforms the original irregular sequence into a high-quality regularized patch representation in a channel-independent manner. This approach effectively adapts to local variations in information density and captures complete semantic information.

3 Methodology

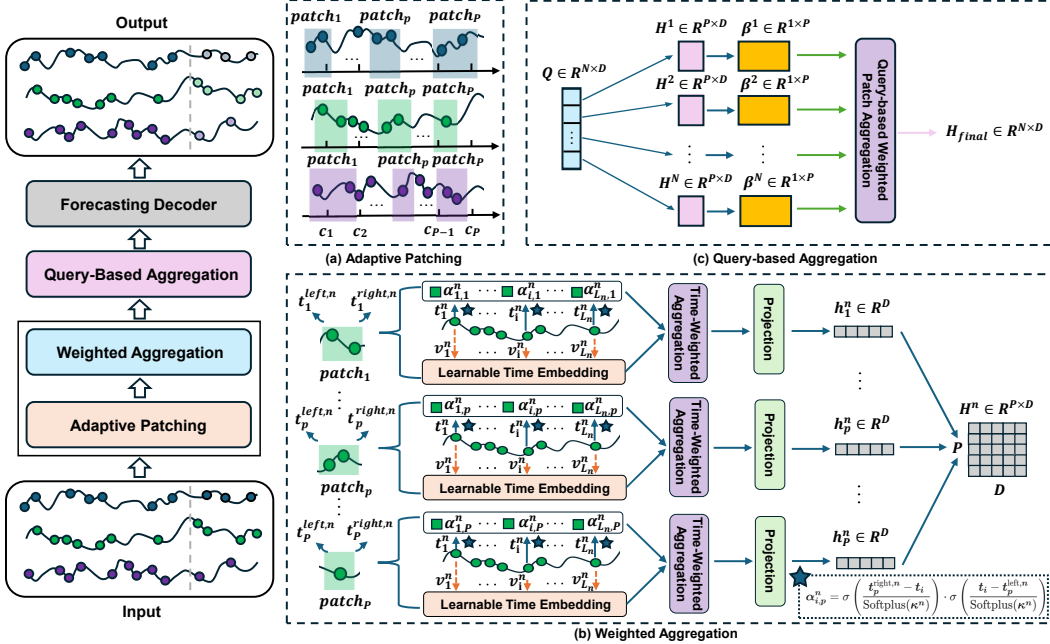


Figure 2: The overall framework of APN, which initially divides each univariate irregular time series into a series of unfixed patches using the *Adaptive Patching Module*. Then the *Weighted Aggregation Module* generates high-quality and regular initial patch representations. Based on the representations, the *Query-based Aggregation Module* is utilized to incorporate contextual information. Finally, the *Forecasting Decoder* outputs the final forecasting results. The *Adaptive Patching Module* and *Weighted Aggregation Module* collectively form the *Time-Aware Patch Aggregation Module*.

3.1 Problem Definition

An Irregular Multivariate Time Series (IMTS) \mathcal{O} consists of N independent univariate sequences $\{o_{1:L_n}^n\}_{n=1}^N$. Each sequence $o_{1:L_n}^n$ comprises L_n observations (t_i^n, v_i^n) , where the intervals between timestamps t_i^n are irregular, and sampling across different variables is typically asynchronous. The IMTS forecasting task is defined as: given historical observations \mathcal{O} and a set of prediction queries for all variables $\mathcal{Q} = \{[q_j^n]_{j=1}^{Q_n}\}_{n=1}^N$, construct and optimize a prediction model $\mathcal{F}(\cdot)$ capable of accurately predicting the future observed values $\hat{\mathcal{V}} = \{[\hat{V}_j^n]_{j=1}^{Q_n}\}_{n=1}^N$ corresponding to each query q_j^n , i.e.:

$$\mathcal{F}(\mathcal{O}, \mathcal{Q}) \rightarrow \hat{\mathcal{V}} \quad (1)$$

3.2 Framework Overview

The overall pipeline of APN is shown in Figure 2. Its core component is the *Time-Aware Patch Aggregation* (TAPA) Module—see Section 3.3, which processes the multivariate irregular sequence in a Channel-Independent manner. Compared with conventional fixed segmentation, TAPA utilizes the *Adaptive Patching* and *Weighted Aggregation*. This design explicitly aims to adapt to the local variations in information density inherent in IMTS and to capture complete semantic information. Then, a concise and efficient *Query-based Aggregation* module—see Section 3.4 generates a representation of historical information for each variable. Finally, this representation is fed into a simple MLP-based *Forecasting decoder* to make predictions—see Section 3.5. In brief, the core advantage of APN stems from the high-quality representations produced by TAPA, which effectively compresses the historical information through adapting to variations in the distribution and concentration of information and preserving complete semantic context, thus APN achieves state-of-the-art performance with a subsequent simple MLP decoder.

3.3 Time-Aware Patch Aggregation (TAPA)

Traditional Fixed-Span Patching [Zhang et al., 2024, Liu et al., 2025], due to the fixed patch boundaries or predefined time spans, struggles to adapt to local variations in the underlying information content and its temporal distribution (referred to as information density), and to capture complete semantic information in IMTS. To overcome this limitation, the TAPA mechanism devises the *Adaptive Patching* and *Weighted Aggregation* to (1) adapt the patching strategy to the local information density variations within each time series, and (2) ensure that crucial semantic information is holistically captured within the generated patches by focusing on the information most important for the prediction task. It efficiently integrates the information in each univariate irregular sequence $X^n = \{(t_i^n, v_i^n)\}_{i=1}^{L_n}$ by transforming it into regularized patch representations $H^n = [h_1^n, \dots, h_P^n]$. This process is performed independently for each variable, accommodating their unique sampling patterns and information distributions.

3.3.1 Adaptive Patching

The *Adaptive Patching* works through dynamically learning the temporal coverage range $[t_p^{left,n}, t_p^{right,n}]$ for each target patch. This dynamic learning of boundaries is the primary mechanism by which TAPA adapts to local information density variations. For instance, in sparsely observed regions that nonetheless contain critical information, the learned patch width (controlled by λ_p^n) might expand to ensure this information is captured, or its position (controlled by δ_p^n) might shift to center on these information-rich sparse points. Conversely, in densely observed regions with redundant information, a patch might become narrower to focus only on the novel or most salient signals, thus avoiding dilution by less informative data. Furthermore, this adaptive process enables the model to determine the content of each patch based on the inherent importance of the data, which is crucial for capturing complete semantic information. Specifically, TAPA learns the left boundary offset δ_p^n and a log-scale parameter λ_p^n representing the patch width:

$$t_p^{left,n} = c_p - \frac{S_{init}}{2} + \delta_p^n, \quad (2)$$

$$t_p^{right,n} = t_p^{left,n} + \exp(\lambda_p^n), \quad (3)$$

where δ_p^n and λ_p^n are learnable parameters, $c_p = (p - 0.5) \cdot (T_{obs}/P)$ and $S_{init} = T_{obs}/P$ denote the reference center points and initial average patch width. For observations highly important for

prediction (i.e., regions with high information density relevant to the task), different patch boundaries are adjusted to accurately cover these crucial regions, ensuring their semantic integrity. While for regions with noise or low information relevance (low information density), boundaries may contract or shift to reduce their coverage, thus preserving the clarity of the extracted semantic information. The dynamic adjustment of boundaries thus constitutes an effective mechanism for adaptively selecting useful information and forming semantically coherent patches based on learned information importance.

3.3.2 Weighted Aggregation

To fully utilize temporal information from observations, the *Learnable Time Embedding* $TE(t_i) \in \mathbb{R}^{D_{te}}$ is first generated for i -th timestamp, which consists of a linear layer for scale and a sine-activated linear layer for periodicity. Then the Learnable Time Embedding is concatenated with the original observed value v_i to form an augmented representation $\tilde{v}_i = \text{Concat}(v_i, TE(t_i))$.

After determining the dynamic coverage range $[t_p^{left,n}, t_p^{right,n}]$ (which has already adapted to local information densities and aimed to cover semantic regions), we employ a query-like *Weighted Aggregation*. This weighting mechanism synergizes with the adaptive boundaries to further refine the captured semantic information by emphasizing the most salient points within each adaptively formed patch. For any observation i (timestamp t_i) of variable n , its relationship $\alpha_{i,p}^n$ to target patch p is defined by a soft window function:

$$\alpha_{i,p}^n = \sigma \left(\frac{t_p^{right,n} - t_i}{\text{Softplus}(\kappa^n)} \right) \cdot \sigma \left(\frac{t_i - t_p^{left,n}}{\text{Softplus}(\kappa^n)} \right), \quad (4)$$

where $\sigma(\cdot)$ is the Sigmoid function, and $\text{Softplus}(\kappa^n)$ is a temperature scaling factor controlled by a learnable scalar parameter κ^n , regulating the smoothness of the soft window boundary transition. Through learning the κ^n , the observations within the dynamically determined patch boundaries are further weighted, where important observations contributing to high local information density receive larger $\alpha_{i,p}^n$ in aggregation, while less relevant observations are down-weighted or filtered out, thus ensuring the completeness and purity of the captured semantic information.

After calculating the relationships between observations and target patches, the aggregated representation \bar{h}_p^n for the p -th patch of variable n can be obtained through a weighted average of the augmented features \tilde{v}_i^n :

$$\bar{h}_p^n = \frac{\sum_i \alpha_{i,p}^n \cdot \tilde{v}_i^n}{\sum_i \alpha_{i,p}^n + \epsilon} \in \mathbb{R}^{1+D_{te}}, \quad (5)$$

where ϵ is a small positive constant to prevent division by zero. Subsequently, we transform $\bar{h}_p^n \in \mathbb{R}^{(1+D_{te})}$ into the uniform hidden representations $h_p^n \in \mathbb{R}^D$ to enhance the expressiveness through a linear projection layer $h_p^n = \text{Linear}_D(\bar{h}_p^n)$.

Through the aforementioned mechanisms, each univariate irregular sequence X^n is efficiently transformed into a refined and structurally regularized patch representation sequence $H^n = [h_1^n, \dots, h_P^n] \in \mathbb{R}^{P \times D}$.

3.4 Query-based Weighted Aggregation

After TAPA generates regularized patch representation sequences $H^n = [h_1^n, \dots, h_P^n] \in \mathbb{R}^{P \times D}$ for each variable, APN employs a concise mechanism to summarize them into a single representation H_c^n , obviating complex inter-sequence transformation modules. To preserve the sequential order of patches, standard positional encodings $PE \in \mathbb{R}^{P \times D}$ are added to H^n , yielding position-aware patch representations $H_{pe}^n = H^n + PE$. Then, to dynamically select and fuse information most relevant to the prediction task, a learnable query vector $q^n \in \mathbb{R}^D$ is introduced for each variable n . This query vector interacts with all P position-aware patches H_{pe}^n , calculating unregularized importance scores s_p^n via dot product, which are then regularized into weight coefficients $\beta^n = [\beta_1^n, \dots, \beta_P^n]$ using the Softmax function. Finally, the representation H_c^n of variable n is obtained by a weighted sum of all

patches $h_{pe,p}^n$:

$$s_p^n = \frac{q^n \cdot (h_{pe,p}^n)^T}{\sqrt{D}} \quad \text{for } p = 1, \dots, P, \quad (6)$$

$$\beta^n = \text{Softmax}(\{s_p^n\}_{p=1}^P), \quad (7)$$

$$H_c^n = \sum_{p=1}^P \beta_p^n h_{pe,p}^n, \quad (8)$$

where the summary representations of all variables $[H_c^1, \dots, H_c^N]$ form the final representation matrix $H_{final} \in \mathbb{R}^{N \times D}$, which is then processed by a layer normalization to stabilize subsequent MLP input. This learnable *Query-based Weighted Aggregation* is concise and efficient, avoiding complex key-value projections or pairwise inter-patch interactions, demonstrating APN’s simple yet effective design.

3.5 Forecasting Decoder

After obtaining the summary historical representation $H_{final}^n \in \mathbb{R}^D$ for each variable n and the target query time point τ_k , APN employs a two-layer MLP decoder for prediction. The decoder takes the concatenation of the variable’s summary representation H_{final}^n and the learnable temporal encoding $TE(\tau_k)$ of the query time point τ_k as input, outputting the predicted value \hat{v}_k^n :

$$\hat{v}_k^n = \text{MLP}(\text{Concat}(H_{final}^n, TE(\tau_k))) \in \mathbb{R} \quad (9)$$

3.6 Loss Function

The overall training objective of the APN model is to minimize the Mean Squared Error (MSE) between predicted and true observed values. For given historical observations \mathcal{O}_{hist} and a set of query time points $\mathcal{T}_{pred} = \{\tau_k\}_{k=1}^H$, the loss function \mathcal{L} is defined as:

$$\mathcal{L} = \frac{1}{N \cdot H} \sum_{n=1}^N \sum_{k=1}^H (\hat{v}_k^n - v_k^n)^2, \quad (10)$$

where v_k^n is the true value of variable n at query time τ_k , and \hat{v}_k^n is the model’s prediction.

4 Experiments

4.1 Setup

Datasets: To comprehensively evaluate the model’s performance, we select four widely-used IMTS datasets, including PhysioNet, MIMIC, Activity, and USHCN. These datasets span multiple domains such as healthcare, biomechanics, and climate science. More details of the benchmark datasets are included in Appendix A.1.

Baselines: To comprehensively evaluate the performance of APN, we compare it with nineteen baseline models. These baseline models can be broadly categorized into the following groups: (1) Regular MTSF models: including DLinear [Zeng et al., 2023], TimesNet [Wu et al., 2023], PatchTST [Nie et al., 2023], Crossformer [Wang et al., 2022], Graph Wavenet [Wu et al., 2019], MTGNN [Wu et al., 2020], StemGNN [Cao et al., 2020], CrossGNN [Huang et al., 2023], and FourierGNN [Yi et al., 2023]. (2) IMTS classification/imputation models: including GRU-D [Che et al., 2018], SeFT [Horn et al., 2020], RainDrop [Zhang et al., 2022], Warpformer [Zhang et al., 2023], and mTAND [Shukla and Marlin, 2021]. (3) IMTSF models: including Latent ODEs [Rubanova et al., 2019], CRU [Schirmer et al., 2022], and Neural Flows [Bilos et al., 2021], T-PATCHGNN [Zhang et al., 2024], and TimeCHEAT [Liu et al., 2025]. For detailed information on the baseline models, please refer to Appendix A.2.

Implementation Details: We implement APN and all related experiments using the PyTorch framework on a server equipped with an Intel(R) Xeon(R) Gold 6326 CPU (@ 2.90GHz) and an NVIDIA GeForce RTX 3090 GPU. For our APN model, we set the hidden dimension D according to

Table 1: Overall performance evaluated by MSE and MAE (mean \pm std). The best-performing and second-best results are highlighted in **bold** and underline, respectively.

Dataset	PhysioNet		MIMIC		Human Activity		USHCN	
Metric	MSE $\times 10^{-3}$	MAE $\times 10^{-2}$	MSE $\times 10^{-2}$	MAE $\times 10^{-2}$	MSE $\times 10^{-3}$	MAE $\times 10^{-2}$	MSE $\times 10^{-1}$	MAE $\times 10^{-1}$
DLinear	41.86 \pm 0.05	15.52 \pm 0.03	4.90 \pm 0.00	16.29 \pm 0.05	4.03 \pm 0.01	4.21 \pm 0.01	6.21 \pm 0.00	3.88 \pm 0.02
TimesNet	16.48 \pm 0.11	6.14 \pm 0.03	5.88 \pm 0.08	13.62 \pm 0.07	3.12 \pm 0.01	3.56 \pm 0.02	5.58 \pm 0.05	3.60 \pm 0.04
PatchTST	12.00 \pm 0.23	6.02 \pm 0.14	3.78 \pm 0.03	12.43 \pm 0.10	4.29 \pm 0.14	4.80 \pm 0.09	5.75 \pm 0.01	3.57 \pm 0.02
Crossformer	6.66 \pm 0.11	4.81 \pm 0.11	2.65 \pm 0.10	9.56 \pm 0.29	4.29 \pm 0.20	4.89 \pm 0.17	5.25 \pm 0.04	3.27 \pm 0.09
Graph Wavenet	6.04 \pm 0.28	4.41 \pm 0.11	2.93 \pm 0.09	10.50 \pm 0.15	2.89 \pm 0.03	3.40 \pm 0.05	5.29 \pm 0.04	3.16 \pm 0.09
MTGNN	6.26 \pm 0.18	4.46 \pm 0.07	2.71 \pm 0.23	9.55 \pm 0.65	3.03 \pm 0.03	3.53 \pm 0.03	5.39 \pm 0.05	3.34 \pm 0.02
StemGNN	6.86 \pm 0.28	4.76 \pm 0.19	1.73 \pm 0.02	7.71 \pm 0.11	8.81 \pm 0.37	6.90 \pm 0.02	5.75 \pm 0.09	3.40 \pm 0.09
CrossGNN	7.22 \pm 0.36	4.96 \pm 0.12	2.95 \pm 0.16	10.82 \pm 0.21	3.03 \pm 0.10	3.48 \pm 0.08	5.66 \pm 0.04	3.53 \pm 0.05
FourierGNN	6.84 \pm 0.35	4.65 \pm 0.12	2.55 \pm 0.03	10.22 \pm 0.08	2.99 \pm 0.02	3.42 \pm 0.02	5.82 \pm 0.06	3.62 \pm 0.07
GRU-D	5.59 \pm 0.09	4.08 \pm 0.05	1.76 \pm 0.03	7.53 \pm 0.09	2.94 \pm 0.05	3.53 \pm 0.06	5.54 \pm 0.38	3.40 \pm 0.28
SeFT	9.22 \pm 0.18	5.40 \pm 0.08	1.87 \pm 0.01	7.84 \pm 0.08	12.20 \pm 0.17	8.43 \pm 0.07	5.80 \pm 0.19	3.70 \pm 0.11
RainDrop	9.82 \pm 0.08	5.57 \pm 0.06	1.99 \pm 0.03	8.27 \pm 0.07	14.92 \pm 0.14	9.45 \pm 0.05	5.78 \pm 0.22	3.67 \pm 0.17
Warpformer	5.94 \pm 0.35	4.21 \pm 0.12	1.73 \pm 0.04	7.58 \pm 0.13	2.79 \pm 0.04	3.39 \pm 0.03	5.25 \pm 0.05	3.23 \pm 0.05
mTAND	6.23 \pm 0.24	4.51 \pm 0.17	1.85 \pm 0.06	7.73 \pm 0.13	3.22 \pm 0.07	3.81 \pm 0.07	5.33 \pm 0.05	3.26 \pm 0.10
Latent-ODE	6.05 \pm 0.57	4.23 \pm 0.26	1.89 \pm 0.19	8.11 \pm 0.52	3.34 \pm 0.11	3.94 \pm 0.12	5.62 \pm 0.03	3.60 \pm 0.12
CRU	8.56 \pm 0.26	5.16 \pm 0.09	1.97 \pm 0.02	7.93 \pm 0.19	6.97 \pm 0.78	6.30 \pm 0.47	6.09 \pm 0.17	3.54 \pm 0.18
Neural Flow	7.20 \pm 0.07	4.67 \pm 0.04	1.87 \pm 0.05	8.03 \pm 0.19	4.05 \pm 0.13	4.46 \pm 0.09	5.35 \pm 0.05	3.25 \pm 0.05
T-PATCHGNN	4.98 \pm 0.08	3.72 \pm 0.03	1.69 \pm 0.03	7.22 \pm 0.09	2.66 \pm 0.03	3.15 \pm 0.02	5.00 \pm 0.04	3.08 \pm 0.04
TimeCHEAT	5.03 \pm 0.07	3.88 \pm 0.03	1.71 \pm 0.02	7.41 \pm 0.10	4.05 \pm 0.10	4.64 \pm 0.07	4.25 \pm 0.07	3.18 \pm 0.05
APN (ours)	4.48 \pm 0.06	3.43 \pm 0.02	1.61 \pm 0.02	6.82 \pm 0.05	2.77 \pm 0.00	3.10 \pm 0.01	4.09 \pm 0.06	2.92 \pm 0.05

different datasets. Specifically, the hidden dimension D is set to 64 for the PhysioNet and USHCN, while it is set to 16 for the Human Activity and MIMIC. The time encoding dimension D_{te} is uniformly set to 10. The number of patches P is adjusted based on the characteristics of the datasets: 20 for PhysioNet, 16 for MIMIC, 75 for Human Activity, and 4 for USHCN. The training batch size is set to 256 for all datasets. The model is trained using the Adam optimizer with an initial learning rate of 1×10^{-2} . We train the model for a maximum of 200 epochs and employ an early stopping strategy with a patience of 50. All experiments are repeated 5 times, and the mean and standard deviation of the performance metrics are reported to ensure the robustness of the results.

4.2 Main results

We compare the APN model with nineteen baseline models on four challenging datasets—see Table 1. We have the following observations: 1) APN achieves leading prediction accuracy across the board. On all datasets, APN achieves optimal or highly competitive forecasting performance. Compared to the second-best performing model, T-PATCHGNN, APN achieves significant reductions in MSE and MAE metrics by approximately 9.63% and 5.24%, respectively. 2) APN demonstrates exceptional cross-domain generalization capability and robustness. Whether on IMTS datasets with different characteristics in healthcare (PhysioNet, MIMIC), biomechanics (Human Activity), or climate science (USHCN), APN consistently performs excellently. The outstanding performance of APN can be attributed to its innovative use of adaptive patching, which generates high-quality and regular initial patch representations. Building on these representations, APN employs a streamlined query module to effectively integrate contextual information, ensuring a lightweight and efficient framework design.

4.3 Ablation Studies

To validate the contributions of each key component of our APN model, we conduct ablation experiments—see Table 2. We have the following observations: 1) *w/o Adaptive Patching*: Replacing the learnable boundaries in TAPA with fixed time windows leads to performance degradation across all datasets, demonstrating the importance of the adaptive boundary learning mechanism. 2) *w/o Weighted Aggregation*: Replacing the time membership-based weighted averaging in TAPA with a simple arithmetic average of observations within the boundaries results in a significant performance drop. This highlights the core value of the time membership weighting strategy in synergizing with dynamic boundaries to further refine information and balance the information density within patches. 3) *w/o Query-Based Patch Aggregation*: Replacing the query-based intra-variable patch aggregation module with a simple linear mapping also leads to a notable performance loss, indicating that even with high-quality initial patch representations, effective context information integration remains crucial.

Table 2: Ablation studies for APN in terms of the best result highlighted in **bold**.

Dataset	PhysioNet		MIMIC		Human Activity		USHCN	
Metric	$MSE \times 10^{-3}$	$MAE \times 10^{-2}$	$MSE \times 10^{-2}$	$MAE \times 10^{-2}$	$MSE \times 10^{-3}$	$MAE \times 10^{-2}$	$MSE \times 10^{-1}$	$MAE \times 10^{-1}$
w/o Adaptive Patching	4.58 ± 0.05	3.45 ± 0.03	1.65 ± 0.02	6.94 ± 0.04	2.78 ± 0.01	3.11 ± 0.00	4.38 ± 0.05	3.07 ± 0.04
w/o Weighted Aggregation	9.92 ± 0.11	5.81 ± 0.07	1.64 ± 0.03	6.96 ± 0.05	4.36 ± 0.12	4.28 ± 0.03	4.19 ± 0.02	2.95 ± 0.03
w/o Query-based Patch Aggregation	9.92 ± 0.10	4.71 ± 0.09	3.57 ± 0.03	11.58 ± 0.10	2.81 ± 0.02	3.18 ± 0.05	4.51 ± 0.04	3.52 ± 0.02
APN (ours)	4.48 ± 0.06	3.43 ± 0.02	1.61 ± 0.02	6.82 ± 0.05	2.77 ± 0.00	3.10 ± 0.01	4.09 ± 0.06	2.92 ± 0.05

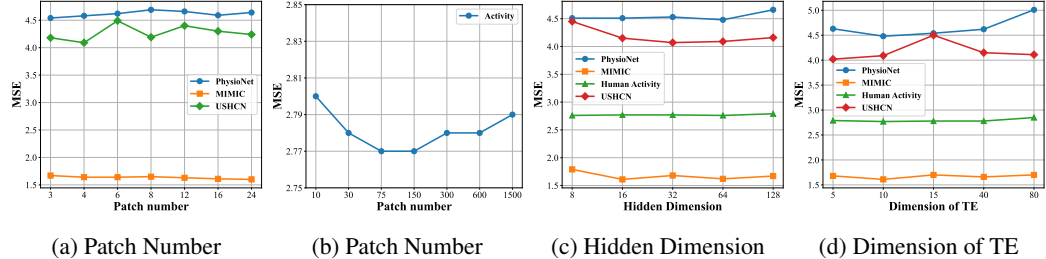


Figure 3: Parameter sensitivity studies of main hyper-parameters in APN

4.4 Parameter Sensitivity

To gain a deeper understanding of the impact of key hyperparameters on the performance of the APN model, we conduct parameter sensitivity analyses, focusing primarily on the number of patches (P), the model’s hidden dimension (D), and the time encoding dimension (D_{te})—see Table 3. We have the following observations: 1) From Figures 3a and 3b, we observe that for most datasets, a larger P does not necessarily lead to better performance. This suggests that an appropriate P value can better balance the capture of local information and model complexity. 2) Figure 3c reveals the impact of the model’s hidden dimension (D). In general, a smaller hidden dimension may already be sufficient to capture effective information, while an excessively large dimension can sometimes lead to a slight performance decline. This indicates that the choice of D should be comprehensively considered based on the scale and sparsity of the dataset. 3) Figure 3d shows the influence of the time encoding dimension (D_{te}). The results indicate that a moderate D_{te} value can provide the model with effective temporal information. An excessively high time encoding dimension may introduce too much noise, interfering with the learning of core features. 4) The APN model exhibits a certain sensitivity to the selection of these core hyperparameters, but it generally achieves competitive results within a reasonable range. In practical applications, appropriate tuning should be performed based on the specific characteristics of the dataset.

4.5 Scalability and Efficiency Analysis

To comprehensively evaluate the potential of APN in practical deployment, we conduct a comparative analysis of computational efficiency and resource consumption between APN and three representative baseline models (TimeCHEAT [Liu et al., 2025], CRU [Schirmer et al., 2022], T-PatchGNN [Zhang et al., 2024]) on the PhysioNet dataset, with the batch size uniformly set to 32—see Figure 4. The results demonstrate that APN exhibits significant advantages across all key efficiency metrics. This is attributed to its core TAPA module, which efficiently generates information-condensed and regularized initial representations. These representations support a highly streamlined information aggregation and prediction architecture, ultimately achieving a lightweight and highly efficient model design.

4.6 Varying Horizon

To further evaluate the robustness of APN under varying combinations of observation history lengths and forecasting horizons, we conduct experiments on the PhysioNet dataset—as shown in Table 3. The results demonstrate that APN exhibits strong predictive capabilities and broad adaptability

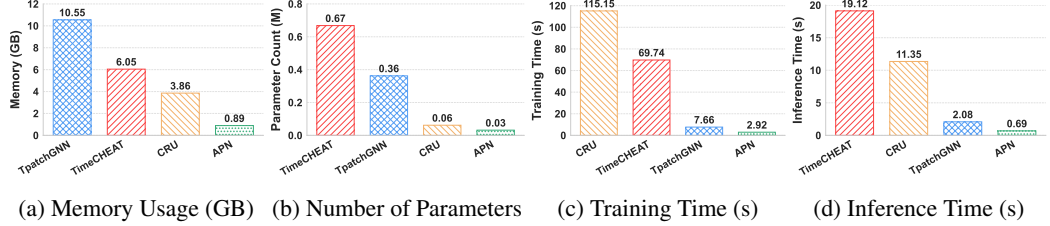


Figure 4: We evaluate the memory usage (GB), number of parameters (M), average training time per epoch (s), and total inference time (s) of APN and three representative baselines for IMTSF. All experiments are conducted on the PhysioNet dataset with a consistent batch size of 32 to ensure fair comparison. A lower value indicates better performance.

Table 3: Performance of varying observation and forecast horizons.

Algorithm	History=3h, Forecast=45h		History=12h, Forecast=36h		History=36h, Forecast=12h		History=45h, Forecast=3h	
	MSE $\times 10^{-3}$	MAE $\times 10^{-2}$	MSE $\times 10^{-3}$	MAE $\times 10^{-2}$	MSE $\times 10^{-3}$	MAE $\times 10^{-2}$	MSE $\times 10^{-3}$	MAE $\times 10^{-2}$
DLLinear	51.82	17.13	43.56	15.73	41.63	15.48	41.23	15.51
TimesNet	57.30	10.70	24.95	7.62	13.57	5.50	13.86	5.65
PatchTST	42.18	13.67	18.56	7.80	9.85	5.11	8.53	4.64
Crossformer	9.48	5.86	8.57	5.70	5.70	4.47	5.33	4.44
Graph Wavenet	9.43	5.86	7.23	4.82	4.71	3.90	4.10	3.73
MTGNN	9.83	5.95	7.48	5.01	5.08	3.99	5.22	4.19
StemGNN	8.70	5.37	7.46	4.84	6.65	4.69	5.47	4.56
CrossGNN	10.44	6.56	7.97	5.37	6.87	4.73	4.80	4.24
FourierGNN	9.59	5.61	7.95	4.99	6.35	4.61	5.37	4.34
GRU-D	8.18	4.99	6.89	4.55	4.42	3.66	4.44	3.79
SeFT	9.78	5.55	9.30	5.41	9.15	5.15	8.76	5.57
RainDrop	10.47	5.72	9.89	5.62	9.70	5.40	9.28	5.62
Warpformer	8.48	5.13	7.57	4.83	5.60	4.09	6.44	4.67
mtAND	8.45	5.23	7.11	4.67	5.71	4.17	5.44	4.33
Latent-ODE	<u>8.25</u>	5.04	7.20	4.69	6.70	4.36	7.10	5.33
CRU	9.20	5.38	9.20	5.31	9.50	5.41	11.60	6.98
Neural Flow	8.30	4.99	8.50	5.27	7.70	4.68	7.40	5.10
T-PATCHGNN	8.01	4.87	6.48	4.19	4.14	3.31	3.69	3.25
TimeCHEAT	9.43	5.41	6.64	4.57	5.26	4.04	2.79	3.35
APN (ours)	8.79	<u>4.90</u>	5.97	3.94	3.91	3.08	2.51	2.65

across multiple "History-Forecast" settings. In scenarios where historical information is relatively sufficient or the prediction span is moderate, APN achieves optimal performance in both MSE and MAE metrics, leading comprehensively. Under extreme settings with extremely limited historical information and long prediction spans, APN's performance is comparable to several strong baseline models, ranking second only to T-PATCHGNN. Considering the significant challenges faced by all models under such extreme sparsity conditions, APN's TAPA mechanism, which relies on learning adaptive features from data, may not fully realize its potential when historical information is scarce. Nevertheless, APN still demonstrates competitive robustness.

5 Conclusion

This paper addresses the challenges of IMTS forecasting by proposing a general and efficient APN. The core of APN lies in its novel TAPA module. Through learned dynamically adjustable patch boundaries and a time-aware weighting strategy, TAPA adaptively transforms irregular sequences into a fixed number of high-quality, regularized patch representations with highly condensed information, operating in a channel-independent manner. Leveraging the superior initial representations generated by TAPA, APN employs an exceptionally lean query module to integrate historical information and completes predictions via a shallow MLP. Extensive experiments on multiple public IMTS benchmark datasets demonstrate that APN significantly outperforms existing state-of-the-art methods in both prediction accuracy and computational efficiency.

References

Zhenjie Yao, Jie Bi, and Yixin Chen. Applying deep learning to individual and community health monitoring data: A survey. *Int. J. Autom. Comput.*, 15(6):643–655, 2018.

Edward De Brouwer, Jaak Simm, Adam Arany, and Yves Moreau. Gru-ode-bayes: Continuous modeling of sporadically-observed time series. In *Advances in Neural Information Processing Systems 32: Annual Conference on Neural Information Processing Systems 2019, NeurIPS 2019, December 8-14, 2019, Vancouver, BC, Canada*, pages 7377–7388, 2019.

Patrick Kidger, James Morrill, James Foster, and Terry J. Lyons. Neural controlled differential equations for irregular time series. In *Advances in Neural Information Processing Systems 33: Annual Conference on Neural Information Processing Systems 2020, NeurIPS 2020, December 6-12, 2020, virtual*, 2020.

Yoo-Geun Ham, Jeong-Hwan Kim, and Jing-Jia Luo. Deep learning for multi-year ENSO forecasts. *Nat.*, 573(7775):568–572, 2019.

Roberto Vio, María Díaz-Trigo, and Paola Andreani. Irregular time series in astronomy and the use of the lomb-scargle periodogram. *Astron. Comput.*, 1:5–16, 2013.

Vijaya Krishna Yalavarthi, Kiran Madhusudhanan, Randolph Scholz, Nourhan Ahmed, Johannes Burchert, Shayan Jawed, Stefan Born, and Lars Schmidt-Thieme. Graffiti: Graphs for forecasting irregularly sampled time series. In *Thirty-Eighth AAAI Conference on Artificial Intelligence, AAAI 2024, Thirty-Sixth Conference on Innovative Applications of Artificial Intelligence, IAAI 2024, Fourteenth Symposium on Educational Advances in Artificial Intelligence, EAAI 2014, February 20-27, 2024, Vancouver, Canada*, pages 16255–16263, 2024.

Weijia Zhang, Chenlong Yin, Hao Liu, Xiaofang Zhou, and Hui Xiong. Irregular multivariate time series forecasting: A transformable patching graph neural networks approach. In *Forty-first International Conference on Machine Learning, ICML 2024, Vienna, Austria, July 21-27, 2024*, 2024.

Jiexi Liu, Meng Cao, and Songcan Chen. Timecheat: A channel harmony strategy for irregularly sampled multivariate time series analysis. In *AAAI-25, Sponsored by the Association for the Advancement of Artificial Intelligence, February 25 - March 4, 2025, Philadelphia, PA, USA*, pages 18861–18869, 2025.

Tian Qi Chen, Yulia Rubanova, Jesse Bettencourt, and David Duvenaud. Neural ordinary differential equations. In *Advances in Neural Information Processing Systems 31: Annual Conference on Neural Information Processing Systems 2018, NeurIPS 2018, December 3-8, 2018, Montréal, Canada*, pages 6572–6583, 2018.

Yulia Rubanova, Tian Qi Chen, and David Duvenaud. Latent ordinary differential equations for irregularly-sampled time series. In *Advances in Neural Information Processing Systems 32: Annual Conference on Neural Information Processing Systems 2019, NeurIPS 2019, December 8-14, 2019, Vancouver, BC, Canada*, pages 5321–5331, 2019.

Alessio Gravina, Daniele Zambon, Davide Bacci, and Cesare Alippi. Temporal graph odes for irregularly-sampled time series. In *Proceedings of the Thirty-Third International Joint Conference on Artificial Intelligence, IJCAI 2024, Jeju, South Korea, August 3-9, 2024*, pages 4025–4034, 2024.

Satya Narayan Shukla and Benjamin M. Marlin. Multi-time attention networks for irregularly sampled time series. In *9th International Conference on Learning Representations, ICLR 2021, Virtual Event, Austria, May 3-7, 2021*, 2021.

Zonghan Wu, Shirui Pan, Fengwen Chen, Guodong Long, Chengqi Zhang, and Philip S. Yu. A comprehensive survey on graph neural networks. *IEEE Trans. Neural Networks Learn. Syst.*, 32(1):4–24, 2021.

Yuqi Chen, Kan Ren, Yansen Wang, Yuchen Fang, Weiwei Sun, and Dongsheng Li. Contiformer: Continuous-time transformer for irregular time series modeling. In *Advances in Neural Information Processing Systems 36: Annual Conference on Neural Information Processing Systems 2023, NeurIPS 2023, New Orleans, LA, USA, December 10 - 16, 2023*, 2023.

Jiawen Zhang, Shun Zheng, Wei Cao, Jiang Bian, and Jia Li. Warpformer: A multi-scale modeling approach for irregular clinical time series. In *Proceedings of the 29th ACM SIGKDD Conference on Knowledge Discovery and Data Mining, KDD 2023, Long Beach, CA, USA, August 6-10, 2023*, pages 3273–3285, 2023.

Dongbin Kim, Jinseong Park, Jaewook Lee, and Hoki Kim. Are self-attentions effective for time series forecasting? In *Advances in Neural Information Processing Systems 38: Annual Conference on Neural Information Processing Systems 2024, NeurIPS 2024, Vancouver, BC, Canada, December 10 - 15, 2024*, 2024.

Ailing Zeng, Muxi Chen, Lei Zhang, and Qiang Xu. Are transformers effective for time series forecasting? In *Thirty-Seventh AAAI Conference on Artificial Intelligence, AAAI 2023, Thirty-Fifth Conference on Innovative Applications of Artificial Intelligence, IAAI 2023, Thirteenth Symposium on Educational Advances in Artificial Intelligence, EAAI 2023, Washington, DC, USA, February 7-14, 2023*, pages 11121–11128, 2023.

Shengsheng Lin, Weiwei Lin, Wentai Wu, Haojun Chen, and Junjie Yang. Sparsesf: Modeling long-term time series forecasting with *1k* parameters. In *Forty-first International Conference on Machine Learning, ICML 2024, Vienna, Austria, July 21-27, 2024*, 2024a.

Shengsheng Lin, Weiwei Lin, Xinyi Hu, Wentai Wu, Ruichao Mo, and Haocheng Zhong. Cyclenet: Enhancing time series forecasting through modeling periodic patterns. In *Advances in Neural Information Processing Systems 38: Annual Conference on Neural Information Processing Systems 2024, NeurIPS 2024, Vancouver, BC, Canada, December 10 - 15, 2024*, 2024b.

Mona Schirmer, Mazin Eltayeb, Stefan Lessmann, and Maja Rudolph. Modeling irregular time series with continuous recurrent units. In *International Conference on Machine Learning, ICML 2022, 17-23 July 2022, Baltimore, Maryland, USA*, volume 162 of *Proceedings of Machine Learning Research*, pages 19388–19405, 2022.

Marin Bilos, Johanna Sommer, Syama Sundar Rangapuram, Tim Januschowski, and Stephan Günemann. Neural flows: Efficient alternative to neural odes. In *Advances in Neural Information Processing Systems 34: Annual Conference on Neural Information Processing Systems 2021, NeurIPS 2021, December 6-14, 2021, virtual*, pages 21325–21337, 2021.

Yuqi Nie, Nam H. Nguyen, Phanwadee Sinthong, and Jayant Kalagnanam. A time series is worth 64 words: Long-term forecasting with transformers. In *The Eleventh International Conference on Learning Representations, ICLR 2023, Kigali, Rwanda, May 1-5, 2023*, 2023.

Wenxiao Wang, Lu Yao, Long Chen, Binbin Lin, Deng Cai, Xiaofei He, and Wei Liu. Crossformer: A versatile vision transformer hinging on cross-scale attention. In *The Tenth International Conference on Learning Representations, ICLR 2022, Virtual Event, April 25-29, 2022*, 2022.

Haixu Wu, Tengge Hu, Yong Liu, Hang Zhou, Jianmin Wang, and Mingsheng Long. Timesnet: Temporal 2d-variation modeling for general time series analysis. In *The Eleventh International Conference on Learning Representations, ICLR 2023, Kigali, Rwanda, May 1-5, 2023*, 2023.

Zonghan Wu, Shirui Pan, Guodong Long, Jing Jiang, and Chengqi Zhang. Graph wavenet for deep spatial-temporal graph modeling. In *Proceedings of the Twenty-Eighth International Joint Conference on Artificial Intelligence, IJCAI 2019, Macao, China, August 10-16, 2019*, pages 1907–1913, 2019.

Zonghan Wu, Shirui Pan, Guodong Long, Jing Jiang, Xiaojun Chang, and Chengqi Zhang. Connecting the dots: Multivariate time series forecasting with graph neural networks. In *KDD '20: The 26th ACM SIGKDD Conference on Knowledge Discovery and Data Mining, Virtual Event, CA, USA, August 23-27, 2020*, pages 753–763, 2020.

Defu Cao, Yujing Wang, Juanyong Duan, Ce Zhang, Xia Zhu, Congrui Huang, Yunhai Tong, Bixiong Xu, Jing Bai, Jie Tong, and Qi Zhang. Spectral temporal graph neural network for multivariate time-series forecasting. In *Advances in Neural Information Processing Systems 33: Annual Conference on Neural Information Processing Systems 2020, NeurIPS 2020, December 6-12, 2020, virtual*, 2020.

Qihe Huang, Lei Shen, Ruixin Zhang, Shouhong Ding, Binwu Wang, Zhengyang Zhou, and Yang Wang. Crossgnn: Confronting noisy multivariate time series via cross interaction refinement. In *Advances in Neural Information Processing Systems 36: Annual Conference on Neural Information Processing Systems 2023, NeurIPS 2023, New Orleans, LA, USA, December 10 - 16, 2023*, 2023.

Kun Yi, Qi Zhang, Wei Fan, Hui He, Liang Hu, Pengyang Wang, Ning An, Longbing Cao, and Zhendong Niu. Fouriergnn: Rethinking multivariate time series forecasting from a pure graph perspective. In *Advances in Neural Information Processing Systems 36: Annual Conference on Neural Information Processing Systems 2023, NeurIPS 2023, New Orleans, LA, USA, December 10 - 16, 2023*, 2023.

Zhengping Che, Sanjay Purushotham, Kyunghyun Cho, David Sontag, and Yan Liu. Recurrent neural networks for multivariate time series with missing values. *Scientific reports*, 8(1):6085, 2018.

Max Horn, Michael Moor, Christian Bock, Bastian Rieck, and Karsten M. Borgwardt. Set functions for time series. In *Proceedings of the 37th International Conference on Machine Learning, ICML 2020, 13-18 July 2020, Virtual Event*, volume 119 of *Proceedings of Machine Learning Research*, pages 4353–4363, 2020.

Xiang Zhang, Marko Zeman, Theodoros Tsiligkaridis, and Marinka Zitnik. Graph-guided network for irregularly sampled multivariate time series. In *The Tenth International Conference on Learning Representations, ICLR 2022, Virtual Event, April 25-29, 2022*, 2022.

Abdul Fatir Ansari, Alvin Heng, Andre Lim, and Harold Soh. Neural continuous-discrete state space models for irregularly-sampled time series. In *International Conference on Machine Learning, ICML 2023, 23-29 July 2023, Honolulu, Hawaii, USA*, volume 202 of *Proceedings of Machine Learning Research*, pages 926–951, 2023.

Ilan Naiman, N. Benjamin Erichson, Pu Ren, Michael W. Mahoney, and Omri Azencot. Generative modeling of regular and irregular time series data via koopman vae. In *The Twelfth International Conference on Learning Representations, ICLR 2024, Vienna, Austria, May 7-11, 2024*, 2024.

A Detailed Experimental Setup

A.1 Dataset Details

To comprehensively and rigorously evaluate the predictive performance of our proposed APN model, we conduct extensive experiments on four real-world Irregular Multivariate Time Series (IMTS) datasets. These datasets are selected for their widespread use in benchmarking and public availability, representing typical characteristics of IMTS across different domains. Table 4 summarizes the key statistical features of these datasets.

For all datasets, samples are randomly partitioned into training, validation, and test sets, adhering to the standard 60%:20%:20% ratio. Regarding data preprocessing schemes (e.g., missing value handling, normalization methods, timestamp conversion) and prediction task configurations (e.g., historical observation window length, future prediction horizon length), we strictly follow established mainstream experimental protocols, particularly referencing benchmark settings established in related works such as T-PatchGNN [Zhang et al., 2024], to ensure the fairness and comparability of our experimental results. Next, we detail the characteristics of each dataset and its specific application in this study.

Table 4: Dataset statistics.

Dataset	# Variable	Avg # Obs.	Avg Length	Max Length
PhysioNet	41	10.7	75	216
MIMIC	96	1.5	46.1	643
Human Activity	12	30.2	120.6	130
USHCN	5	36.1	163.9	214

- **PhysioNet** [Ansari et al., 2023]: Physionet¹ dataset contains time series data collected from 12,000 ICU patients. Each record details 41 clinical physiological indicators during the first 48 hours after ICU admission, with irregular sampling intervals and a significant amount of missing values. Following the standard settings of [Ansari et al., 2023, Rubanova et al., 2019], we use the observation data from the first 24 hours after each patient’s admission to predict their physiological indicator values for the subsequent 24 hours. Original data and access methods are available on the official PhysioNet website.
- **MIMIC** [Naiman et al., 2024]: MIMIC² dataset is a large, publicly available database of de-identified critical care medical information. Following the commonly used preprocessing procedures in studies such as [Bilos et al., 2021, Naiman et al., 2024], we filter and process records to obtain 23,457 patient entries. Each record contains 96 irregularly sampled clinical variables from the first 48 hours after patient admission, also exhibiting significant irregularity and missingness. The experimental task is set to utilize data from the first 24 hours to predict variable values within the subsequent 24 hours. Access to this dataset requires certification and adherence to data use agreements via PhysioNet.
- **Human Activity** [Zhang et al., 2023]: Human Activity³ dataset comprises 12 motion-related variables (e.g., 3D acceleration, 3D gyroscope) recorded by sensors worn on different body parts (wrist, chest, ankle) of test subjects, with irregular sampling times. To construct IMTS samples suitable for forecasting tasks, we segment the original long sequences into clips of 4000 milliseconds and use the observation data from the first 3000 milliseconds to predict sensor readings for the next 1000 milliseconds. Through this process, we obtain a total of 5,400 IMTS samples to evaluate the model’s capability in biomechanical signal prediction.
- **USHCN** [Ansari et al., 2023]: The USHCN dataset⁴ contains daily data for 5 core climate variables (daily maximum temperature, daily minimum temperature, daily precipitation, daily snow depth, daily snowfall) recorded from 1,114 weather stations across the United States between 1996 and 2000. This dataset is characterized by its long time span and

¹<https://archive.physionet.org/challenge/2012/>

²<https://physionet.org/content/mimiciii/1.4/>

³<https://archive.ics.uci.edu/dataset/196/localization+data+for+person+activity>

⁴<https://www.osti.gov/biblio/1394920>

naturally occurring spatial and temporal irregularities and data missingness due to station maintenance, equipment failure, etc. Following the experimental setup of [Ansari et al., 2023, Rubanova et al., 2019], we process the data for the task of using climate records from the past 24 months to predict climate conditions for the next 1 month, generating a total of 26,736 IMTS samples to test the model’s predictive performance on long-period, sparse climate data.

A.2 Baseline Model Details

To construct a comprehensive and convincing benchmark for the IMTS forecasting task, we integrate nineteen relevant baseline models for meticulous comparison. In selecting and evaluating these baseline models, we adhere to established mainstream experimental protocols [Zhang et al., 2024]. Specifically, we adapt state-of-the-art models from regular multivariate time series (RMTS) forecasting, IMTS classification, and IMTS imputation for the current IMTS forecasting task by appropriate modifications (e.g., altering the output layer for prediction tasks and incorporating timestamps and mask information as input features).

To ensure fairness and reliability of comparison, for some baseline models that have been rigorously evaluated in recent related works such as T-PatchGNN [Zhang et al., 2024], we prioritize referencing and reporting their publicly available optimal experimental results. For other models, or when evaluation under specific experimental settings is required, we reproduce them based on their official open-source implementations within a unified and consistent experimental framework. During reproduction, we conduct exploratory searches around the hyperparameter configurations recommended in the original papers and select the optimal parameter combinations based on performance on the validation set to report their best performance. This approach, combining references to existing SOTA results with careful reproduction, aims to provide a broad yet rigorous performance reference system for our APN model.

Next, we detail the core ideas, key mechanisms, and reference code sources for each baseline model:

Regular MTSF models:

- **DLinear** [Zeng et al., 2023]: Models the trend and periodicity/residual terms of a time series using two independent single-layer linear networks, respectively, and then sums them to obtain the final prediction. Its design philosophy is that simple and effective linear models remain competitive in many forecasting tasks. Code Reference: <https://github.com/cure-lab/LTSF-Linear>
- **TimesNet** [Wu et al., 2023]: Innovatively transforms one-dimensional time series into two-dimensional tensors to capture multi-periodicity. It identifies major periods via Fourier transform and reshapes sub-sequences of different periods into 2D tensors (with period-based "columns" and intra-period "rows"), then uses a 2D convolutional network to extract features, aiming to uniformly handle series with complex periodicities. Code Reference: <https://github.com/thumt/TimesNet>
- **PatchTST** [Nie et al., 2023]: Segments each univariate time series into fixed-length non-overlapping patches, which serve as input tokens for a Transformer. It employs a Channel Independence strategy, modeling each variable independently, and learns temporal dependencies through a shared Transformer backbone. Code Reference: <https://github.com/yuqinie/PatchTST>
- **Crossformer** [Wang et al., 2022]: A Transformer variant with a two-stage attention mechanism. The first stage captures intra-sequence temporal dependencies through dimension embedding and temporal self-attention; the second stage explicitly models interactions between different variables (dimensions) via an innovative Dimension-Segment-Wise Attention. Code Reference: <https://github.com/Thinklab-AI/Crossformer>
- **Graph Wavenet** [Wu et al., 2019]: Combines Graph Convolutional Networks (GCN) with stacked dilated causal convolutions. It uses an adaptive adjacency matrix to learn dynamic spatial dependencies between variables and efficiently captures long-range temporal dependencies through dilated convolutions. Code Reference: <https://github.com/mnzhan/Graph-WaveNet>

- **MTGNN** [Wu et al., 2020]: Proposes a general framework comprising a graph learning module, a graph convolution module, and a temporal convolution module. Its graph learning module adaptively infers unidirectional relationships between variables through node embedding and metric learning. Code Reference: <https://github.com/nnzhan/MTGNN>
- **StemGNN** [Cao et al., 2020]: First transforms spatio-temporal graph data into the spectral domain (via Graph Fourier Transform and Discrete Fourier Transform), then designs modules in the spectral domain to capture spatial and temporal dependencies, and finally obtains predictions through inverse transformation. Code Reference: <https://github.com/microsoft/StemGNN>
- **CrossGNN** [Huang et al., 2023]: To handle noise in multivariate time series, this model first generates multiple time series copies at different noise levels (data augmentation), then performs information interaction and feature refinement via cross-scale GNN and cross-variable GNN. Code Reference: <https://github.com/hqh0728/CrossGNN>
- **FourierGNN** [Yi et al., 2023]: Treats multivariate time series from a pure graph perspective, where each time series is a node on the graph, and different time points are node features. Graph neural operations are performed in the Fourier domain to achieve prediction. Code Reference: <https://github.com/aikunyi/FourierGNN>

IMTS classification/imputation models:

- **GRU-D** [Che et al., 2018]: An improved GRU model that models the influence of observation intervals through an introduced learnable time decay term and handles missing values via feature-level imputation to dynamically update hidden states. Code Reference: <https://github.com/zhiyongc/GRU-D>
- **SeFT (Set Functions for Time Series)** [Horn et al., 2020]: Treats observation points of an irregular time series (typically as (time, value, variable ID) tuples) as an unordered set and models them using set functions like Deep Sets, naturally handling irregularity and variable length. Code Reference: <https://github.com/mims-harvard/Raindrop>
- **RainDrop** [Zhang et al., 2022]: Models irregularly sampled data from a sensor network as a graph, where each observation point is a node. It captures spatio-temporal dependencies via graph attention networks and temporal attention mechanisms, generating interpolations or predictions for arbitrary query time points. Code Reference: <https://github.com/mims-harvard/Raindrop>
- **Warpformer** [Zhang et al., 2023]: A multi-scale modeling approach for irregular clinical time series. Its core is the introduction of a learnable dynamic time warping module that adaptively aligns time series of different scales and sampling rates to a reference timeline before feeding them into a Transformer for representation learning. Code Reference: <https://github.com/imJiawen/Warpformer>
- **mTAND** [Shukla and Marlin, 2021]: A multi-time attention network designed for irregularly sampled time series. It learns embedding representations for continuous timestamps and generates fixed-length context representations for variable-length input sequences, used for interpolation or classification. Code Reference: <https://github.com/reml-lab/mTAN>

IMTSF models:

- **Latent ODEs** [Rubanova et al., 2019]: Compresses historical observation sequences (potentially variable-length and irregular) into a latent initial state via an RNN encoder, then evolves this state in latent space using a Neural ODE (an ordinary differential equation parameterized by a neural network), and finally generates predictions through a decoder. Code Reference: <https://github.com/YuliaRubanova/latent-ode>
- **CRU (Continuous Recurrent Units)** [Schirmer et al., 2022]: Proposes a continuous-time recurrent unit whose hidden state evolution is driven by a linear stochastic differential equation, with irregularly spaced observation updates handled via Kalman filtering theory. Code Reference: <https://github.com/boschresearch/Continuous-Recurrent-Units>
- **Neural Flows** [Bilos et al., 2021]: Reformulates the solving process of Neural ODEs as a continuous normalizing flow, aiming to improve numerical solution efficiency and stability by directly modeling the solution function of the ODE rather than its derivative. Code Reference: <https://github.com/mbilos/neural-flows-experiments>

- **T-PATCHGNN** [Zhang et al., 2024]: Specifically designed for IMTS forecasting. Its core is to transform irregular univariate sequences into time-aligned patch sequences via a transformable patching method, then combine Transformers to capture intra-patch temporal dependencies and utilize time-adaptive graph neural networks to model dynamic inter-variable dependencies. Code Reference: <https://github.com/usail-hkust/t-PatchGNN>
- **TimeCHEAT** [Liu et al., 2025]: Proposes a channel harmony strategy, employing channel-dependent graph convolutions within patches and channel-independent Transformers between patches to balance information processing across different channels. Code Reference: <https://github.com/Alrash/TimeCHEAT>

For all baseline models, we endeavor to use the official implementations provided by their authors or widely recognized community implementations. Regarding hyperparameter settings, we first refer to the recommendations in the original papers and then adjust them based on performance on the validation set to ensure fair comparison.

B Limitation

Although the APN method demonstrates its effectiveness, several aspects warrant further exploration:

- **Limited Scope of Validation Datasets:** APN’s current validation primarily focuses on specific types of real-world datasets. Its adaptability and performance on more diverse domains, such as high-frequency financial data, industrial data with strong periodicities, or traffic flow with complex covariates, require further investigation to fully assess its generalization capabilities.
- **Performance in Extreme Scenarios:** In situations with exceptionally short observation histories and very long prediction horizons, APN’s performance can be suboptimal. This is potentially because the data-driven adaptive mechanism struggles to converge effectively with extremely scarce information. Future work could explore incorporating prior knowledge or regularization to enhance robustness under such data-sparse conditions.